



Research Paper



Families of efficient low order processed composition methods

S. Blanes^a, F. Casas^b, A. Escorihuela-Tomàs^{c,*}^a *Universitat Politècnica de València, Instituto de Matemática Multidisciplinar, 46022-Valencia, Spain*^b *Departament de Matemàtiques and IMAC, Universitat Jaume I, 12071-Castellón, Spain*^c *Departament de Matemàtiques, Universitat Jaume I, 12071-Castellón, Spain*

ARTICLE INFO

MSC:
65L05
65P10

Keywords:

Composition methods
Effective error
Processing technique
Splitting
Hamiltonian systems

ABSTRACT

New families of composition methods with processing of order 4 and 6 are presented and analyzed. They are specifically designed to be used for the numerical integration of differential equations whose vector field is separated into three or more parts which are explicitly solvable. The new schemes are shown to be more efficient than previous state-of-the-art splitting methods.

1. Introduction

Structure-preserving numerical integration methods are nowadays a common tool in many areas of physics, chemistry and computational mathematics [2,11]. Among them, splitting methods constitute a natural option when the differential system can be separated into two parts, so that each of them is explicitly integrable [7,18]. Suppose the vector field f in

$$\dot{x} \equiv \frac{dx}{dt} = f(x), \quad x(t_0) = x_0 \in \mathbb{R}^D \quad (1.1)$$

can be split into two parts, $f(x) = f_1(x) + f_2(x)$, so that each subproblem

$$\dot{x} = f_i(x), \quad x(t_0) = x_0, \quad i = 1, 2$$

is explicitly solvable, with solution $x(t) = \varphi_t^{[i]}(x_0)$. Then, the composition

$$\chi_h = \varphi_h^{[2]} \circ \varphi_h^{[1]} \quad (1.2)$$

provides a first-order approximation to the exact flow φ_h of (1.1):

$$\chi_h(x_0) = \varphi_h(x_0) + \mathcal{O}(h^2), \quad \text{as } h \rightarrow 0, \quad (1.3)$$

whereas the palindromic composition

* Corresponding author.

E-mail addresses: serblaza@imm.upv.es (S. Blanes), Fernando.Casas@mat.uji.es (F. Casas), alescori@uji.es (A. Escorihuela-Tomàs).

Table 1

Fourth- and sixth-order symmetric (palindromic) composition methods of the form (1.8). They correspond to the splitting schemes S_6 and S_{10} of [9, Table 2], respectively.

BM ₆ ^[4] (order 4)	
$\alpha_1 = 0.0792036964311957$	$\alpha_2 = 0.1303114101821663$
$\alpha_3 = 0.22286149586760773$	$\alpha_4 = -0.36671326904742574$
$\alpha_5 = 0.32464818868970624$	$\alpha_6 = 0.10968847787674973$
BM ₁₀ ^[6] (order 6)	
$\alpha_1 = 0.0502627644003922$	$\alpha_2 = 0.0985536835006498$
$\alpha_3 = 0.31496061692769417$	$\alpha_4 = -0.44734648269547816$
$\alpha_5 = 0.49242637248987586$	$\alpha_6 = -0.42511876779769087$
$\alpha_7 = 0.23706391397812188$	$\alpha_8 = 0.19560248860005314$
$\alpha_9 = 0.34635818985072686$	$\alpha_{10} = -0.36276277925434486$

$$S_h^{[2]} = \varphi_{h/2}^{[1]} \circ \varphi_h^{[2]} \circ \varphi_{h/2}^{[1]}, \tag{1.4}$$

known as the Strang splitting method, is of second-order. Higher-order schemes can be constructed as

$$\psi_h = \varphi_{hb_s}^{[2]} \circ \varphi_{ha_s}^{[1]} \circ \dots \circ \varphi_{hb_1}^{[2]} \circ \varphi_{ha_1}^{[1]}$$

if the coefficients a_j, b_j are conveniently chosen so as to satisfy the required order conditions [11,18].

There are problems, however, where f has to be split into more than two terms for each part to be explicitly integrable, i.e., $f(x) = \sum_{i=1}^n f_i(x), n \geq 3$. In that case, method (1.3) generalizes to

$$\chi_h = \varphi_h^{[n]} \circ \varphi_h^{[n-1]} \circ \dots \circ \varphi_h^{[2]} \circ \varphi_h^{[1]} \tag{1.5}$$

(or any other permutation of the sub-flows $\varphi_h^{[j]}$), leading to a first-order approximation. This is also the case of the adjoint of χ_h , defined as $\chi_h^* = (\chi_{-h})^{-1}$, namely

$$\chi_h^* = \varphi_h^{[1]} \circ \varphi_h^{[2]} \circ \dots \circ \varphi_h^{[n-1]} \circ \varphi_h^{[n]},$$

whereas the composition $\chi_{h/2} \circ \chi_{h/2}^*$ leads to a second-order approximation $S_h^{[2]}$, the generalization of scheme (1.4) to this setting. Higher order integrators can be constructed as compositions of $S_h^{[2]}$. Thus, in particular, the 4th-order scheme

$$S_h^{[4]} = S_{\alpha_1 h}^{[2]} \circ S_{\alpha_2 h}^{[2]} \circ S_{\alpha_1 h}^{[2]}, \quad \text{with} \quad \alpha_1 = \frac{1}{2 - 2^{1/3}}, \quad \alpha_2 = 1 - 2\alpha_1, \tag{1.6}$$

is very popular in applications [28,6], although it has large truncation errors and a short stability interval. Alternatively, the 4th-order scheme

$$\psi_h = S_{\alpha_1 h}^{[2]} \circ S_{\alpha_1 h}^{[2]} \circ S_{\alpha_3 h}^{[2]} \circ S_{\alpha_1 h}^{[2]} \circ S_{\alpha_1 h}^{[2]}, \quad \text{with} \quad \alpha_1 = \frac{1}{4 - 4^{1/3}}, \quad \alpha_3 = 1 - 4\alpha_1,$$

first proposed in [22] and analyzed in detail in [17], is much more efficient than (1.6), even if it requires more computational effort per step, whereas palindromic compositions of the form

$$\psi_h = S_{\alpha_m h}^{[2]} \circ S_{\alpha_{m-1} h}^{[2]} \circ \dots \circ S_{\alpha_2 h}^{[2]} \circ S_{\alpha_1 h}^{[2]} \quad \text{with} \quad (\alpha_1, \dots, \alpha_m) \in \mathbb{R}^m \tag{1.7}$$

and $\alpha_{m+1-i} = \alpha_i$, lead to efficient integrators of order $r > 6$ [11].

The most general situation corresponds to integrators of the form

$$\psi_h = \chi_{\alpha_{2s} h} \circ \chi_{\alpha_{2s-1} h}^* \circ \dots \circ \chi_{\alpha_2 h} \circ \chi_{\alpha_1 h}^*, \quad \text{with} \quad (\alpha_1, \dots, \alpha_{2s}) \in \mathbb{R}^{2s} \tag{1.8}$$

verifying in addition the condition $\alpha_{2s+1-i} = \alpha_i$ to preserve time-symmetry. In fact, methods (1.7) constitute a particular case of (1.8) when $S_h^{[2]}$ is the Strang map (1.4). Among the most efficient 4th- and 6th-order methods of this class we can mention the schemes introduced by Blanes and Moan [9], denoted here as BM₆^[4] and BM₁₀^[6], respectively. They have $s = 6$ and $s = 10$ stages, and their coefficients are collected in Table 1. The main truncation error of the 4th-order scheme BM₆^[4] is around 500 times smaller than the error of method (1.6), thus compensating its higher computational cost per step. For future reference, this scheme reads explicitly

$$BM_6^{[4]} : \quad \chi_{\alpha_1 h} \circ \chi_{\alpha_2 h}^* \circ \chi_{\alpha_3 h} \circ \chi_{\alpha_4 h}^* \circ \chi_{\alpha_5 h} \circ \chi_{\alpha_6 h}^* \circ \chi_{\alpha_6 h} \circ \chi_{\alpha_5 h}^* \circ \chi_{\alpha_4 h} \circ \chi_{\alpha_3 h}^* \circ \chi_{\alpha_2 h} \circ \chi_{\alpha_1 h}^* \tag{1.9}$$

Actually, schemes BM₆^[4] and BM₁₀^[6] are constructed in [9] as splitting methods when f is separated into two parts. Specifically, if χ_h is taken as (1.2), then scheme (1.8) can be rewritten as

Table 2
Schemes of effective order four and six of the form (1.8). They correspond to methods P_6^4 and P_6^6 of [5, Table 5], respectively. With an appropriate processor, they render 4th- and 6th-order composition schemes.

BCM ₆ ^[4] (effective order 4)	
$\alpha_1 = \alpha_2 = \alpha_3 = \alpha_4$	$\alpha_4 = 0.1341940158122142$
$\alpha_5 = -0.3141940158122142$	$\alpha_6 = 0.27741795256335733$
BCM ₉ ^[6] (effective order 6)	
$\alpha_1 = \alpha_2 = \alpha_3 = \alpha_4 = \alpha_5$	$\alpha_5 = 0.1106570871853300$
$\alpha_6 = -0.2854111127287940$	$\alpha_7 = 0.2138498496192465$
$\alpha_8 = -0.3402583791791715$	$\alpha_9 = 0.35853420636206895$

$$\psi_h = \varphi_{a_{s+1}h}^{[1]} \circ \varphi_{b_s h}^{[2]} \circ \varphi_{a_s h}^{[1]} \circ \dots \circ \varphi_{a_2 h}^{[1]} \circ \varphi_{b_1 h}^{[2]} \circ \varphi_{a_1 h}^{[1]}, \tag{1.10}$$

where $a_1 = \alpha_1$, and for $j = 1, \dots, s$,

$$a_{j+1} = \alpha_{2j} + \alpha_{2j+1}, \quad b_j = \alpha_{2j-1} + \alpha_{2j} \tag{1.11}$$

(with $\alpha_{2s+1} = 0$). Conversely, any integrator of the form (1.10) satisfying the condition $\sum_{j=1}^{s+1} a_j = \sum_{j=1}^s b_j$ can be expressed in the form (1.8), as shown in [16].

The aim of this paper is to construct new classes of 4th- and 6th-order composition methods that are even more efficient for problems that can be expressed as the sum of three or more explicitly integrable terms. These are built by applying the processing technique. Although a detailed study of composition methods with processing was carried out in [5] and methods up to order 12 were presented there, we think methods of low order require an additional treatment to improve their overall efficiency due to their relevance in practical applications. This is the subject of the present work, where we present new families of processed composition schemes with a better performance than the *de facto* state-of-the-art numerical integrators of Table 1. This claim is further substantiated by numerical tests on different problems. Although the new schemes are specifically designed and optimized for systems separable into $n \geq 3$ parts, the case $n = 2$ is also contemplated. Furthermore, the new schemes are also compared with the most efficient processed methods of order 4 and 6 obtained in [5], whose coefficients (for the kernel) are collected in Table 2.

2. Processed composition methods

Processed (or corrected) methods are of the form

$$\hat{\psi}_h = \pi_h \circ \psi_h \circ \pi_h^{-1}. \tag{2.1}$$

The integrator ψ_h is called the *kernel* and the (near-identity) map π_h is the *processor* or *corrector*. The method ψ_h is said to be of effective order r if a processor exists such that $\hat{\psi}_h$ is of (conventional) order r [10]. Note that, since

$$\hat{\psi}_h^N = \pi_h \circ \psi_h^N \circ \pi_h^{-1},$$

applying $\hat{\psi}_h$ over N steps with constant h only involves N evaluations of the kernel, whereas π_h^{-1} is computed only at the beginning and π_h when output is desired [15,8].

Processed integrators have shown to be very efficient in a variety of systems, ranging from near-integrable problems to Hamiltonian systems separable into kinetic and potential energy [15,27,8]. This is due essentially to the fact that the kernel has to satisfy a much reduced set of order conditions (in other words, some of the order conditions can be fulfilled by the processor) and therefore they require less computational effort than a conventional method of the same order.

The derivation and analysis of the effective order conditions for kernels of the form (1.8) has been done in [5], where kernels of effective orders 4 and 6 have also been proposed (for order $r > 6$ it is more advantageous to consider directly palindromic compositions of the form (1.7)). Here we briefly summarize the treatment when $r \leq 6$ and construct new families of schemes.

The corresponding analysis can be carried out with the help of the Lie formalism. To proceed, we introduce the Lie derivative F associated with f in (1.1), and defined as

$$F g(x) = \left. \frac{d}{dh} \right|_{h=0} g(\varphi_h(x))$$

for each smooth function $g : \mathbb{R}^D \rightarrow \mathbb{R}$ and $x \in \mathbb{R}^D$, that is,

$$F g(x) = f(x) \cdot \nabla g(x). \tag{2.2}$$

Then, the h -flow of Eq. (1.1) verifies [11,21]

$$g(\varphi_h(x)) = e^{hF} g(x),$$

Table 3
Particular basis of \mathcal{L}_j , $1 \leq j \leq 7$, taken in this work.

\mathcal{L}_j	Basis of \mathcal{L}_j		
\mathcal{L}_1	$E_{1,1} = Y_1$		
\mathcal{L}_2	$E_{2,1} = Y_2$		
\mathcal{L}_3	$E_{3,1} = Y_3$	$E_{3,2} = [Y_1, Y_2]$	
\mathcal{L}_4	$E_{4,1} = Y_4$	$E_{4,2} = [Y_1, Y_3]$	$E_{4,3} = [Y_1, E_{3,2}]$
\mathcal{L}_5	$E_{5,1} = Y_5$	$E_{5,2} = [Y_1, Y_4]$	$E_{5,3} = [Y_1, E_{4,2}]$
	$E_{5,4} = [Y_1, E_{4,3}]$	$E_{5,5} = [Y_2, Y_3]$	$E_{5,6} = [Y_2, E_{3,2}]$
\mathcal{L}_6	$E_{6,1} = Y_6$	$E_{6,2} = [Y_1, Y_5]$	
	$E_{6,3+i} = [Y_1, E_{5,2+i}]$	$i = 0, \dots, 4$	
	$E_{6,8} = [Y_2, Y_4]$	$E_{6,9} = [Y_2, E_{4,2}]$	
\mathcal{L}_7	$E_{7,1} = Y_7$	$E_{7,2} = [Y_1, Y_6]$	
	$E_{7,3+j} = [Y_1, E_{6,2+j}]$	$j = 0, \dots, 7$	
	$E_{7,11} = [Y_2, Y_5]$	$E_{7,12+k} = [Y_2, E_{5,2+k}]$	$k = 0, \dots, 4$
	$E_{7,17} = [Y_3, Y_4]$	$E_{7,18} = [Y_3, E_{4,2}]$	

where e^{hF} is defined as a series of linear differential operators

$$e^{hF} = \sum_{k=0}^{\infty} \frac{h^k}{k!} F^k.$$

Analogously, for the basic method χ_h of (1.5), one can associate a series of linear operators so that [6]

$$g(\chi_h(x)) = e^{Y(h)} g(x), \quad \text{with} \quad Y(h) = \sum_{k \geq 1} h^k Y_k$$

with $Y_1 = F$, whereas for its adjoint one has $g(\chi_h^*(x)) = e^{-Y(-h)} g(x)$. In consequence, the integrator (1.8) has associated a series $\Psi(h)$ of differential operators given by

$$\Psi(h) = e^{-Y(-h\alpha_1)} e^{Y(h\alpha_2)} \dots e^{-Y(-h\alpha_{2s-1})} e^{Y(h\alpha_{2s})}, \tag{2.3}$$

in the sense that $g(\psi_h(x)) = \Psi(h)g(x)$. Successive applications of the Baker–Campbell–Hausdorff formula [23] in (2.3) allow us to formally express $\Psi(h)$ as only one exponential,

$$\Psi(h) = \exp(K(h)), \quad \text{with} \quad K(h) = \sum_{j \geq 1} h^j K_j, \tag{2.4}$$

the terms $h^j K_j \in \mathcal{L}_j$ for each $j \geq 1$ and $\mathcal{L} = \bigoplus_{j \geq 1} \mathcal{L}_j$ is the graded free Lie algebra generated by $\{Y_1, Y_3, Y_5, \dots\}$ [20]. For the particular basis of \mathcal{L}_j , $j \leq 7$, collected in Table 3, the operator $K(h)$ associated with a consistent time-symmetric method (1.8) reads

$$K(h) = hF + h^3(k_{3,1}E_{3,1} + k_{3,2}E_{3,2}) + h^5 \sum_{\ell=1}^6 k_{5,\ell} E_{5,\ell} + h^7 \sum_{\ell=1}^{18} k_{7,\ell} E_{7,\ell} + \mathcal{O}(h^9), \tag{2.5}$$

where $k_{n,\ell}$ are polynomials of degree n in the coefficients α_j . Due to the time-symmetry, only odd order terms appear in (2.5) [21].

As for the processor, when the kernel is time-symmetric, it can be chosen such that $\pi_{-h} = \pi_h$. In that case, its associated series of differential operators can be expressed as $\Pi(h) = \exp(P(h))$, with $P(-h) = P(h)$ [4]. Explicitly,

$$P(h) = h^2 p_{2,1} E_{2,1} + h^4(p_{4,1} E_{4,1} + p_{4,2} E_{4,2} + p_{4,3} E_{4,3}) + \mathcal{O}(h^6). \tag{2.6}$$

In consequence, the series of operators associated to the processed method (2.1) is

$$\hat{\Psi}(h) = e^{\hat{F}(h)} = \Pi(h)^{-1} \Psi(h) \Pi(h) = e^{-P(h)} e^{K(h)} e^{P(h)}, \tag{2.7}$$

so that

$$\begin{aligned} \hat{F}(h) &= e^{-\text{ad}_{P(h)}} K(h) = K(h) - [P(h), K(h)] + \frac{1}{2}[P(h), [P(h), K(h)]] + \dots \\ &= F + h^3(f_{3,1}E_{3,1} + f_{3,2}E_{3,2}) + h^5 \sum_{\ell=1}^6 f_{5,\ell} E_{5,\ell} + \mathcal{O}(h^7), \end{aligned} \tag{2.8}$$

where $f_{i,j}$ depend on $k_{\ell,m}$ and $p_{k,n}$. The method is of order r if $f_{i,j} = 0$ for all $1 < i \leq r$. This leads to a set of restrictions on the coefficients of the kernel (the effective order conditions), whereas $P(h)$ is obtained by fixing its coefficients $p_{k,n}$ so as to satisfy the remaining conditions. Since the kernel is time-symmetric, we can choose without loss of generality $p_{2n-1,j} = 0$, $n \geq 1$ [8]. All these conditions up to order 7 are collected in Table 4.

Table 4
Order conditions for the kernel ψ_h and processor π_h up to order r when the time-symmetric kernel ($k_{2n,l} = 0$) is expressed in the basis of Table 3. In that case, $p_{2n-1,j} = 0, n = 1, 2, 3$.

r	Eff. order conditions	Processor conditions
1	$k_{1,1} = 1$	
3	$k_{3,1} = 0$	$p_{2,1} = k_{3,2}$
5	$k_{5,1} = k_{5,5} = 0$ $k_{5,6} = -\frac{1}{2}k_{3,2}^2$	$p_{4,1+i} = k_{5,2+i}, \quad i = 0, 1, 2$
7	$k_{7,i} = 0, \quad i = 1, 11, 15, 17, 18$ $k_{7,16} = \frac{1}{6}k_{3,2}^3$ $k_{7,10+j} = -k_{3,2}k_{5,j}, \quad j = 2, 3, 4$	$p_{6,1+l} = k_{7,2+l}, \quad l = 0, \dots, 5$ $p_{6,7} = k_{7,8} - \frac{1}{2}k_{3,2}k_{5,4}$ $p_{6,8} = k_{7,9} - \frac{1}{2}k_{3,2}k_{5,2} \quad p_{6,9} = k_{7,10} - \frac{1}{2}k_{3,2}k_{5,3}$

Table 5
Theoretical efficiencies of s -stage kernels $\psi_s^{[4]}$ of effective order 4.

s	$E_{\text{ef}}^{(5)}$	$E_{\text{ef}}^{(7)}$	$E_{\text{ef}}^{(9)}$	1-norm
3	2.2753	2.5675	2.6384	4.4048
4	1.5470	1.7567	1.8304	2.8523
5	1.3142	1.5034	1.5775	2.3177
6	1.2026	1.3984	1.4852	2.0417
7	1.1389	1.3220	1.4207	1.8710
8	1.1001	1.2961	1.4061	1.7543
9	1.0778	1.2662	1.3903	1.6672

3. Processed methods of order 4

3.1. Construction of kernels

According with Table 4, two order conditions have to be solved by a palindromic kernel of the form (1.8) to achieve effective order 4. In other words, $s \geq 2$. As noticed previously [5], with $s = 2$ there are only complex solutions, so that more stages have to be introduced and, consequently, one has free parameters. In these circumstances, some criterion has to be adopted to make an appropriate selection of the free parameters. A standard strategy consists in minimizing the non-correctable error terms at order 5, since they cannot be removed by a processor anyway. In our case, these terms can be grouped into the function

$$\mathcal{E}_5 \equiv \left(k_{5,1}^2 + k_{5,5}^2 + (k_{5,6} + \frac{1}{2}k_{3,2}^2)^2 \right)^{1/2}, \tag{3.1}$$

and also corresponds to the 2-norm of the vector $(f_{5,1}, \dots, f_{5,6})$ of the coefficients $f_{5,j}$ in the series (2.8), once the coefficients $p_{i,j}$ are chosen according with the prescription of Table 4 up to $i = 4$. To take into account the computational cost corresponding to a kernel (1.8) with s stages, the following function, with $r = 5$, is used to measure the relative efficiency of each method [5]:

$$E_{\text{ef}}^{(r)} = s \mathcal{E}_r^{1/(r-1)}. \tag{3.2}$$

In addition, we also keep track of the non-correctable error terms at orders 7 and 9 with the same function (with $r = 7$ and $r = 9$), and the size of the coefficients, as measured by the 1-norm of the vector $(\alpha_1, \dots, \alpha_{2s})$. In this way we hope to keep higher-order errors under control.

We have analyzed compositions with $3 \leq s \leq 9$ stages. Specifically, we have solved the effective order conditions and expressed the solutions in terms of the free parameters. Then, we have written the corresponding function \mathcal{E}_5 in terms of these parameters and explored systematically the parameter domain to find its local minima. Finally, we have taken the set of values which provide the smallest value for \mathcal{E}_5 . In this way we get the coefficient collected in Table 6, with the theoretical efficiencies gathered in Table 5.

For comparison with the schemes we construct here, the kernel of the processed method $\text{BCM}_6^{[4]}$ of Table 2 has the value $E_{\text{ef}}^{(5)} = 1.3432$, whereas the corresponding value for the scheme $\text{BM}_6^{[4]}$ of Table 1 is 1.5829.

Notice that by including more basic maps in the composition it is possible to reduce the value of $E_{\text{ef}}^{(r)}$, and that errors at higher order also reduce accordingly. Although several values of the coefficients provide essentially the same (minimum) value for \mathcal{E}_5 , the observed pattern closely follows the rule of thumb formulated by McLachlan [17] for kernels of the form (1.7) and effective order 4: (i) set the maximum possible number of outer stages in (1.7) equal to eliminate free parameters; (ii) find the solution of the effective order conditions with the remaining parameters; (iii) either use the resulting method as it is or take it as the starting point for further minimize the main error term.

It is shown in [17] that the minimum effective error is obtained for $s = 19$, which is precisely the same pattern observed here: $E_{\text{ef}}^{(5)}$ achieves its minimum value ≈ 1 when $s = 19$.

Methods with $s = 8, 9$ in Table 6 have been obtained by applying the rule of thumb, but considering two and three free parameters, respectively, for further optimization. Once the free parameters have been selected the remaining coefficients can be determined with

Table 6
Coefficients of time-symmetric kernels of the form (1.8) of effective order 4 and s stages, $3 \leq s \leq 9$.

$s = 3, \psi_3^{[4]}$	
$\alpha_1 = \alpha_2 = \frac{1}{6}(2 + 2^{-1/3} + 2^{1/3})$	$\alpha_3 = \frac{1}{2} - 2\alpha_1$
$s = 4, \psi_4^{[4]}$	
$\alpha_1 = 0.32175$	$\alpha_2 = -0.46308$
$\alpha_3 = 0.3257797788491148$	$\alpha_4 = 0.3155502211508852$
$s = 5, \psi_5^{[4]}$	
$\alpha_1 = \alpha_2 = 0.2014$	$\alpha_3 = 0.2136$
$\alpha_4 = -0.3294322555468401$	$\alpha_5 = 0.2130322555468401$
$s = 6, \psi_6^{[4]}$	
$\alpha_1 = 0.15$	$\alpha_2 = 0.15$
$\alpha_3 = 0.14353$	$\alpha_4 = 0.1592$
$\alpha_5 = -0.2604319166278054$	$\alpha_6 = 0.1577019166278054$
$s = 7, \psi_7^{[4]}$	
$\alpha_1 = 0.1174$	$\alpha_2 = 0.1158$
$\alpha_3 = 0.1227$	$\alpha_4 = 0.112$
$\alpha_5 = 0.12685$	$\alpha_6 = -0.2177553177818525$
$\alpha_7 = 0.1230053177818525$	
$s = 8, \psi_8^{[4]}$	
$\alpha_1 = \alpha_2 = \alpha_3 = \alpha_4 = 0.09755$	$\alpha_5 = 0.09$
$\alpha_6 = 0.1061$	$\alpha_7 = -0.1885819261107769$
$\alpha_8 = 0.1022819261107769$	
$s = 9, \psi_9^{[4]}$	
$\alpha_1 = \alpha_2 = \dots = \alpha_7 = 0.082576$	
$\alpha_8 = -0.1668033908821750$	$\alpha_9 = 0.0887713908821750$

arbitrary precision. Here, for convenience, we only show the first 16 digits. We notice that, although the value of $E_{\text{ef}}^{(r)}$ diminishes indeed with s , it does so more slowly (for instance, for $s = 10$ it is approximately 1.06), so that in practice we restrict ourselves to $s \leq 9$.

3.2. Testing the kernels

A simple technique can be used to test the effective order and the relative efficiency of the kernels proposed, before attempting to construct a processor to form the whole integrator, a task that becomes increasingly difficult with the order. To proceed, let us consider the linear $d \times d$ matrix system

$$\dot{U} = (A_1 + A_2 + A_3)U, \quad U(0) = I, \tag{3.3}$$

with exact solution $U_{\text{ex}} = e^{(A_1+A_2+A_3)t}$, determine the trace of the approximation rendered by the kernel and compare $\text{tr}(\hat{\psi}_h)$ with $\text{tr}(U_{\text{ex}})$ at some final time to get an estimate of the error and efficiency that this particular kernel can achieve by processing. We take $A_j, j = 1, 2, 3$, as 50×50 matrices whose entries are chosen randomly from a normal distribution. In addition, to illustrate the role that the basic scheme may play in the overall performance of the method, we take two different choices for χ_h , namely a composition of the exact flow of each sub-part,

$$\chi_h = e^{hA_3} e^{hA_2} e^{hA_1} \tag{3.4}$$

and the first-order approximation

$$\chi_h = (I + hA_3)(I + hA_2)(I + hA_1), \tag{3.5}$$

in which case $\chi_h^* = (I - hA_1)^{-1}(I - hA_2)^{-1}(I - hA_3)^{-1}$. Fig. 1a corresponds to one particular instance of the first case, and Fig. 1b corresponds to the second. Here kernels of Table 6 are tested, together with $\text{BM}_6^{[4]}$ and the kernel of method $\text{BCM}_6^{[4]}$ (Table 2). Whereas there is a good deal of variability in the efficiency exhibited by the different schemes with the choice (3.4) depending on the particular matrices A_j , this is not the case of (3.5): in all examples we have tested, the efficiency closely follows the pattern shown in Table 5.

3.3. Construction of the processor

To have a complete integrator we must obtain a processor π_h in (2.1) once a particular kernel has been chosen. This in principle would require determining the exact flow of the infinite series (2.6). For an easier implementation, however, it is more convenient to construct an approximation to π_h as a composition of the same form as the kernel. In our case it would be enough to fix conditions

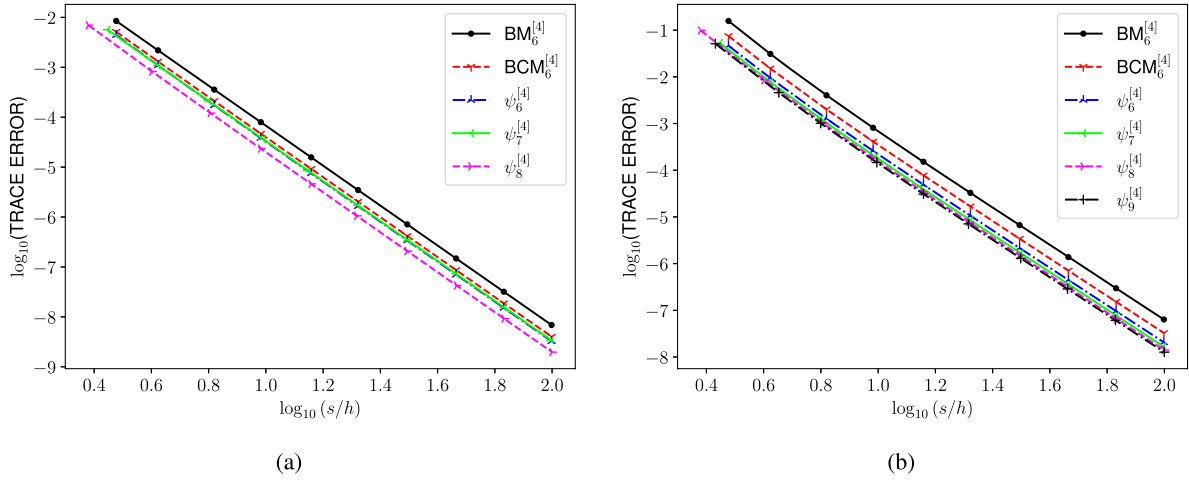


Fig. 1. Error in the trace obtained by kernels of effective order 4 collected in Table 6, together with method $BM_6^{[4]}$ and the kernel of $BCM_6^{[4]}$ when they are applied to the linear system (3.3) at final time $t_f = 10$. (a): basic scheme χ_h taken as (3.4); (b): χ_h given by (3.5).

on $p_{i,j}$ in (2.6) up to order 3, but the overall error is reduced if in addition all the conditions are satisfied up to order 5, as previously explained. In other words, we fix

$$p_{1,1} = p_{3,1} = p_{3,2} = 0, \quad p_{2,1} = k_{3,2},$$

$$p_{4,1} = k_{5,2}, \quad p_{4,2} = k_{5,3}, \quad p_{4,3} = k_{5,4}$$

for a particular kernel, and then construct an approximation of the form

$$\pi_h \approx \pi^{(s,4)} \equiv \chi_{\beta_7 h}^* \circ \chi_{\beta_6 h} \circ \chi_{\beta_5 h}^* \circ \chi_{\beta_4 h} \circ \chi_{\beta_3 h}^* \circ \chi_{\beta_2 h} \circ \chi_{\beta_1 h}^*, \tag{3.6}$$

assuming that the corresponding equations have real solutions. Then, we approximate the inverse map π_h^{-1} by

$$\pi_h^{-1} \approx \chi_{-\beta_1 h} \circ \chi_{-\beta_2 h}^* \circ \chi_{-\beta_3 h} \circ \chi_{-\beta_4 h}^* \circ \chi_{-\beta_5 h} \circ \chi_{-\beta_6 h}^* \circ \chi_{-\beta_7 h}.$$

As explained in [1,3], one can also replace π_h^{-1} by the adjoint π_h^* and obtain an approximation up to the same order. In that case, the integrator after N steps reads

$$\pi_h \circ \psi_h^N \circ \pi_h^*$$

and is also time-symmetric if ψ_h is so, although it cannot be obtained as a N -fold composition of a one-step map [1]. In consequence, we take

$$\pi_h^* \approx \chi_{\beta_1 h} \circ \chi_{\beta_2 h}^* \circ \chi_{\beta_3 h} \circ \chi_{\beta_4 h}^* \circ \chi_{\beta_5 h} \circ \chi_{\beta_6 h}^* \circ \chi_{\beta_7 h}.$$

By applying this strategy, we have determined a processor for each kernel of Table 6 (except for ψ_3 , given its poor efficiency). The overall methods read as

$$\hat{\psi}^{[s,4]} = \pi^{(s,4)} \circ \psi_s^{[4]} \circ (\pi^{(s,4)})^*, \tag{3.7}$$

where s denotes the number of stages of the kernel.

4. Processed methods of order 6

A similar procedure can be carried out to construct processed composition methods of order 6. In this case one has 5 effective order conditions, so that the kernel involves at least $s = 5$ stages. Methods with $s \leq 10$ have been obtained in [5] by applying the previous rule of thumb. They are more efficient than the standard scheme $BM_{10}^{[6]}$ of Table 1 on a number of examples. Proceeding analogously as in the case of order 4, we build new kernels by minimizing the objective function $E_{ef}^{(7)}$. This is done by exploring the space of parameters and identifying local minima of \mathcal{E}_7 for $5 \leq s \leq 11$. The coefficients of the most promising schemes we have found are collected in Table 8, leading to the following efficiencies shown in Table 7.

We should stress that the kernel with $s = 5$ stages also corresponds to a composition (1.7). For comparison, the standard 6th-order method $BM_{10}^{[6]}$ of Table 1 has $E_{ef}^{(7)} = 3.5855$, whereas the kernel $BCM_9^{[6]}$ has $E_{ef}^{(7)} = 2.2144$. It is worth remarking that the most efficient schemes we have found with $s = 10$ and $s = 11$ correspond precisely to a particular case of the rule of thumb. Moreover,

Table 7
Theoretical efficiencies of s -stage kernels $\psi_s^{[6]}$ of effective order 6.

s	$E_{\text{ef}}^{(7)}$	$E_{\text{ef}}^{(9)}$	1-norm
5	5.1053	6.2573	9.6024
6	3.1347	3.6818	5.7329
7	2.5170	2.9862	4.3759
8	2.2193	2.6388	3.6553
9	2.0686	2.4786	3.2417
10	1.9488	2.3345	2.9099
11	1.8718	2.2560	2.6935

Table 8
Coefficients of time-symmetric kernels of the form (1.8) of effective order 6 with s stages, $5 \leq s \leq 11$.

$s = 5, \psi_5^{[6]}$	
$\alpha_1 = 1.1983882307745148$	$\alpha_2 = -1.0753056449710827$
$\alpha_3 = -1.0753056449710827$	$\alpha_4 = 0.7261115295838254$
$\alpha_5 = 0.7261115295838252$	
$s = 6, \psi_6^{[6]}$	
$\alpha_1 = 0.35796564117377453$	$\alpha_2 = 0.3041155195721355$
$\alpha_3 = 0.3544845132692152$	$\alpha_4 = -0.5776359154029904$
$\alpha_5 = -0.6055964252788016$	$\alpha_6 = \frac{2}{3}$
$s = 7, \psi_7^{[6]}$	
$\alpha_1 = 0.2$	$\alpha_2 = 0.2102$
$\alpha_3 = 0.2076682089468185$	$\alpha_4 = 0.2483663566422618$
$\alpha_5 = -0.4108957823061926$	$\alpha_6 = -0.4330744093869198$
$\alpha_7 = 0.4777356261040321$	
$s = 8, \psi_8^{[6]}$	
$\alpha_1 = 0.1535$	$\alpha_2 = 0.146$
$\alpha_3 = 0.1535$	$\alpha_4 = 0.1564865138360776$
$\alpha_5 = 0.1777546764340215$	$\alpha_6 = -0.3260392072026447$
$\alpha_7 = -0.3377852074639321$	$\alpha_8 = 0.3765832243964778$
$s = 9, \psi_9^{[6]}$	
$\alpha_1 = 0.1145$	$\alpha_2 = 0.116$
$\alpha_3 = 0.117$	$\alpha_4 = 0.1115$
$\alpha_5 = 0.1319890385474292$	$\alpha_6 = 0.1512264299418584$
$\alpha_7 = -0.2763628586973695$	$\alpha_8 = -0.2840658003186326$
$\alpha_9 = 0.3182131905267144$	
$s = 10, \psi_{10}^{[6]}$	
$\alpha_1 = \dots = \alpha_7 = 0.1008383848350010$	
$\alpha_8 = \alpha_9 = -0.2387378667702656$	
$\alpha_{10} = 0.2716070396955245$	
$s = 11, \psi_{11}^{[6]}$	
$\alpha_1 = \dots = \alpha_8 = 0.0852884432504611$	
$\alpha_9 = \alpha_{10} = -0.2116830704463290$	
$\alpha_{11} = 0.2410585948889692$	

these schemes correspond precisely to compositions of the form (1.7). A careful exploration of the region of free parameters has not provided solutions with a better efficiency.

Concerning the processor, one has to solve 23 equations to achieve order 6, so we approximate π_h by a composition of the form (3.6), $\pi^{(s,6)} = \chi_{\beta_{23}h}^* \circ \chi_{\beta_{22}h} \circ \dots \circ \chi_{\beta_1h}^*$. Among all the real solutions obtained, we take the one with the minimum 1-norm of the vector $(\beta_1, \dots, \beta_{23})$. The overall method is now denoted as

$$\hat{\psi}^{[s,6]} = \pi^{(s,6)} \circ \psi_s^{[6]} \circ (\pi^{(s,6)})^* \tag{4.1}$$

and methods with $5 \leq s \leq 11$ have been constructed.

We have also explored kernels of order 8, but all the schemes we have been able to construct correspond indeed to compositions of a time-symmetric second order basic method.

5. Numerical experiments

Next we test some of the previous processed methods for the numerical integration of the equations describing the motion of a particle in an electromagnetic field, and the motion around a Reissner–Nordström black hole. In the first case, the system is split into three parts, whereas in the second one has to consider five parts. In this respect, as noted in [19], choosing the right sequence of basic maps when forming χ_h is of the utmost importance. In fact, the numerical experiments carried out in [19] show that the overall efficiency of the scheme may vary significantly with the ordering. For this reason, it is recommended to test different sequences to identify the most efficient for a given problem.

Several codes implementing the previous schemes for the two problems at hand are available at

<https://doi.org/10.5281/zenodo.8375196>.

Specifically, the interested reader can find there the coefficients β_j of the processor for methods of order 4 and 6, eqs. (3.7) and (4.1), together with two new processors for the 4th- and 6th-order proposed in [5] and collected in Table 2 and the codes generating the figures included in this section.

5.1. Motion of a charged particle under Lorentz force

The evolution of a particle of mass m and charge q in a external electromagnetic field (in the non-relativistic limit) is modeled by the equation

$$m \ddot{\mathbf{x}} = q(\mathbf{E} + \dot{\mathbf{x}} \times \mathbf{B}), \tag{5.1}$$

which can also be written as a first-order system:

$$\begin{aligned} \dot{\mathbf{x}} &= \mathbf{v} \\ \dot{\mathbf{v}} &= \frac{q}{m} \mathbf{E} + \omega \mathbf{b} \times \mathbf{v}. \end{aligned} \tag{5.2}$$

Here $\omega = -qB/m$ is the local cyclotron frequency, $B = \|\mathbf{B}\|$ and $\mathbf{b} = \mathbf{B}/B$ is the unit vector in the direction of the magnetic field. In the following, we assume that both \mathbf{E} and \mathbf{B} depend only on the position variables \mathbf{x} .

System (5.2) can be split into three parts in such a way that each subpart is explicitly solvable, and preserve volume in phase space (\mathbf{x}, \mathbf{v}) [13,14]. Specifically, if we define $y = (\mathbf{x}, \mathbf{v})^\top$, then (5.2) can be expressed as

$$\begin{aligned} \dot{y} &= \frac{d}{dt} \begin{pmatrix} \mathbf{x} \\ \mathbf{v} \end{pmatrix} = \begin{pmatrix} \mathbf{v} \\ 0 \end{pmatrix} + \begin{pmatrix} 0 \\ \frac{q}{m} \mathbf{E}(\mathbf{x}) \end{pmatrix} + \begin{pmatrix} 0 \\ \omega(\mathbf{x}) \mathbf{b}(\mathbf{x}) \times \mathbf{v} \end{pmatrix}, \\ &= f^{[A]}(y) + f^{[B]}(y) + f^{[C]}(y), \end{aligned} \tag{5.3}$$

with exact solutions given by

$$\varphi_t^{[A]} : \begin{cases} \mathbf{x}(t) = \mathbf{x}_0 + t \mathbf{v}_0 \\ \mathbf{v}(t) = \mathbf{v}_0 \end{cases} \quad \varphi_t^{[B]} : \begin{cases} \mathbf{x}(t) = \mathbf{x}_0 \\ \mathbf{v}(t) = \mathbf{v}_0 + t \frac{q}{m} \mathbf{E}(\mathbf{x}_0) \end{cases} \quad \varphi_t^{[C]} : \begin{cases} \mathbf{x}(t) = \mathbf{x}_0 \\ \mathbf{v}(t) = e^{t\omega_0 \hat{\mathbf{b}}_0} \mathbf{v}_0 \end{cases} \tag{5.4}$$

in terms of $\omega_0 \equiv \omega(\mathbf{x}_0)$ and $\hat{\mathbf{b}}_0 \equiv \hat{\mathbf{b}}(\mathbf{x}_0)$, with

$$\hat{\mathbf{b}}(\mathbf{x}) = \begin{pmatrix} 0 & -b_3(\mathbf{x}) & b_2(\mathbf{x}) \\ b_3(\mathbf{x}) & 0 & -b_1(\mathbf{x}) \\ -b_2(\mathbf{x}) & b_1(\mathbf{x}) & 0 \end{pmatrix}.$$

In practice, as in [13], we use the expression

$$\exp(t\omega_0 \hat{\mathbf{b}}_0) \mathbf{v}_0 = \mathbf{v}_0 + \sin(t\omega_0) \hat{\mathbf{b}}_0 \mathbf{v}_0 + (1 - \cos(t\omega_0)) \hat{\mathbf{b}}_0^2 \mathbf{v}_0$$

for computing $\varphi_t^{[C]}$, and consider a static, non-uniform electromagnetic field

$$\mathbf{E} = -\nabla V = \frac{\alpha}{r^3} (x \mathbf{e}_x + y \mathbf{e}_y), \quad \mathbf{B} = \nabla \times \mathbf{A} = r \mathbf{e}_z, \tag{5.5}$$

derived from the potentials

$$V = \frac{\alpha}{r}, \quad \mathbf{A} = \frac{r^2}{3} \mathbf{e}_\theta,$$

respectively, in cylindrical coordinates (r, θ, z) . The parameter α is used to parametrize the scalar potential. Then, both the angular momentum and energy

$$L = r^2 \dot{\theta} + \frac{r^3}{3}, \quad H = \frac{1}{2} \|\mathbf{v}\|^2 + \frac{\alpha}{r}$$

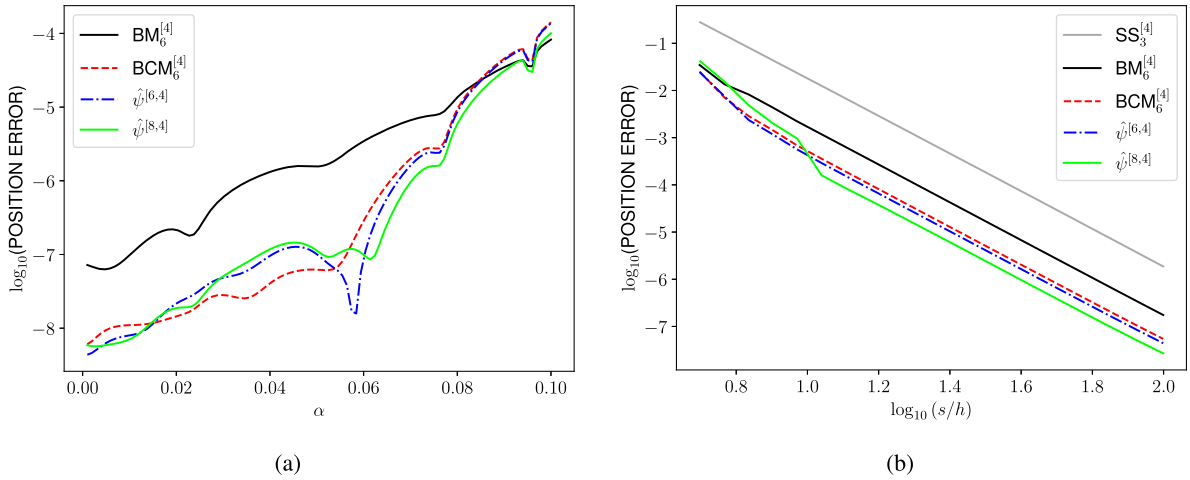


Fig. 2. Motion of a charged particle under Lorentz force. (a) Maximum position error for different values of the parameter α and for various 4th-order methods at the final time $t_f = 200$, evaluated with the same computational cost $s/h = 40$. (b) Efficiency diagram for different 4th-order methods with $\alpha = 0.07$ and $t_f = 200$.

are invariants of the problem.

For the simulations we take $q = -1$, $m = 1$, initial position $\mathbf{x}_0 = (0, -1, 0)^T$ and initial velocity $\mathbf{v}_0 = (0.1, 0.01, 0)$ [13]. In our first experiment we integrate until the final time $t_f = 20$ with the 4th-order processed methods $\hat{\psi}^{[6,4]}$ and $\hat{\psi}^{[8,4]}$ (cf. eqs. (3.7) and (4.1)) and values of α in the interval $(0, 1/10)$. As basic scheme we choose the Lie–Trotter splitting

$$\chi_h = \varphi_h^{[A]} \circ \varphi_h^{[B]} \circ \varphi_h^{[C]}. \tag{5.6}$$

We determine the error in phase space at the final time with each integrator by taking as reference solution the output generated by the standard routine DOP853 [12]. The results are depicted in Fig. 2a, where the errors committed by the standard method $\text{BM}_6^{[4]}$ and the processed scheme $\text{BCM}_6^{[4]}$ are also shown. The step size h is chosen in such a way that all integrators require the same computational cost.

Fig. 2b corresponds to an efficiency diagram obtained by methods $\text{BM}_6^{[4]}$, $\text{BCM}_6^{[4]}$ and the new processed schemes $\hat{\psi}^{[6,4]}$ and $\hat{\psi}^{[8,4]}$ when $\alpha = 0.07$ at the final time $t_f = 200$. Notice that the processed schemes provide more accurate results with the same computational effort. For comparison, we have also depicted the result achieved by the triple jump composition (1.6), $\text{SS}_3^{[4]}$.

Figs. 3a and 3b show the results achieved, for the same problem, initial conditions and final integration time, by the following 6th-order schemes: $\text{BM}_{10}^{[6]}$ (Table 1), $\text{BCM}_9^{[6]}$ (Table 2 with the new processor), $\hat{\psi}^{[8,6]}$ and $\hat{\psi}^{[10,6]}$. Here again the new processed scheme is more efficient when high accuracy is desired. We also include for comparison the result achieved by the most efficient 7-stage 6th-order symmetric composition of 2nd-order schemes proposed in [28], $\text{SS}_7^{[6]}$.

Finally, Fig. 4 shows the non-trivial effects on the overall error of the different orderings in the basic scheme χ_h for several values of α .

5.2. Particle around a Reissner–Nordström black hole

A Schwarzschild black hole with charge Q is known as a Reissner–Nordström black hole. The motion of a test particle around this black hole is described by the Hamiltonian [26]:

$$H = \frac{-1}{2\left(1 - \frac{2}{r} + \frac{Q^2}{r^2}\right)} E^2 + \frac{1}{2} \left(1 - \frac{2}{r} + \frac{Q^2}{r^2}\right) p_r^2 + \frac{1}{2} \frac{p_\theta^2}{r^2} + \frac{L^2}{2r^2 \sin^2 \theta}. \tag{5.7}$$

Here r and θ correspond to the radial and angular coordinates of the particle, p_r and p_θ are their conjugate momenta, and E and L are the energy and angular momentum of the particle, respectively.

This Hamiltonian can be separated into five explicitly integrable parts, namely [26]

$$H = H_A + H_B + H_C + H_D + H_E,$$

with

$$H_A = \frac{-1}{2\left(1 - \frac{2}{r} + \frac{Q^2}{r^2}\right)} E^2 + \frac{L^2}{2r^2 \sin^2 \theta}, \quad H_B = \frac{1}{2} p_r^2,$$

$$H_C = -\frac{1}{r} p_r^2, \quad H_D = \frac{p_\theta^2}{2r^2}, \quad H_E = \frac{Q^2 p_r^2}{2r^2},$$

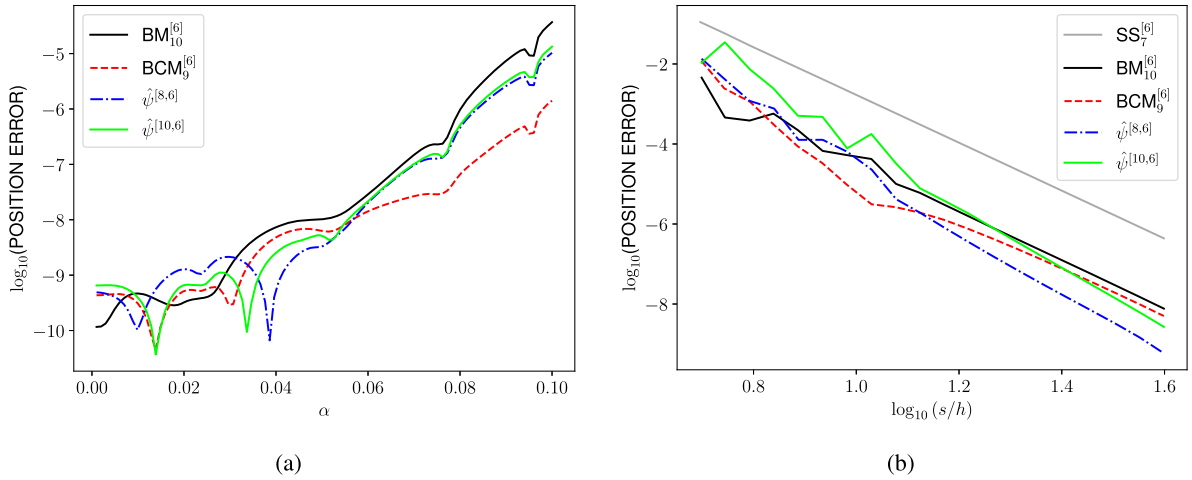


Fig. 3. Motion of a charged particle under Lorentz force. (a) Maximum position error for different values of the parameter α and for various 6th-order methods at the final time $t_f = 200$, evaluated with the same computational cost $s/h = 40$. (b) Efficiency diagram for different 6th-order methods with $\alpha = 0.04$ and $t_f = 200$.

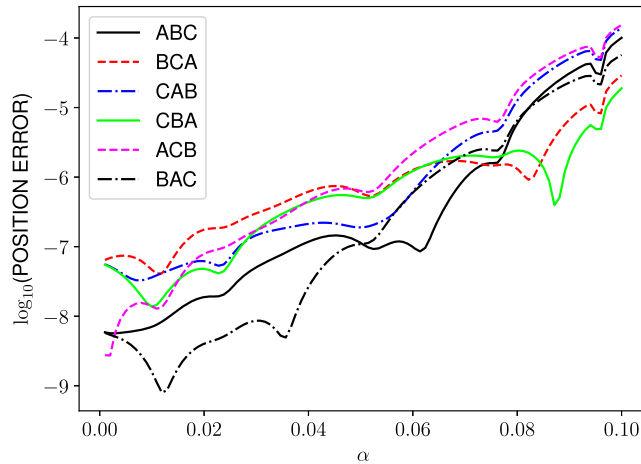


Fig. 4. Motion of a charged particle under Lorentz force. Maximum position error for the method $\hat{\psi}^{[8,4]}$ for different values of the parameter α with all possible orderings of the first-order method χ_h . The simulation was conducted with $s/h = 40$ and $t_f = 200$.

whose flows read explicitly

$$\begin{aligned}
 \varphi_\tau^{[A]} : \begin{cases} r(\tau) = r_0 \\ p_r(\tau) = p_{r0} + \tau \left(\frac{L^2}{r_0^3 \sin^2 \theta_0} - \frac{E^2}{(r_0 - 2)^2} \right) \\ \theta(\tau) = \theta_0 \\ p_\theta(\tau) = p_{\theta0} + \tau \frac{L^2 \cos \theta_0}{r_0^2 \sin^3 \theta_0} \end{cases} & \quad \varphi_\tau^{[B]} : \begin{cases} r(\tau) = r_0 + \tau p_{r0} \\ p_r(\tau) = p_{r0} \\ \theta(\tau) = \theta_0 \\ p_\theta(\tau) = p_{\theta0} \end{cases} \\
 \varphi_\tau^{[C]} : \begin{cases} r(\tau) = \left(\frac{(r_0^2 - 3\tau p_{r0})^2}{r_0} \right)^{1/3} \\ p_r(\tau) = p_{r0} \left(\frac{(r_0^2 - 3\tau p_{r0})}{r_0^2} \right)^{1/3} \\ \theta(\tau) = \theta_0 \\ p_\theta(\tau) = p_{\theta0} \end{cases} & \quad \varphi_\tau^{[D]} : \begin{cases} r(\tau) = r_0 \\ p_r(\tau) = p_{r0} + \tau \frac{p_{\theta0}^2}{r_0^3} \\ \theta(\tau) = \theta_0 + \tau \frac{p_{r0}^2}{r_0^2} \\ p_\theta(\tau) = p_{\theta0} \end{cases} & \quad \varphi_\tau^{[E]} : \begin{cases} r(\tau) = r_0 + \tau p_{r0} \frac{Q^2}{r^2} \\ p_r(\tau) = p_{r0} + \tau \frac{Q^2 p_{r0}^2}{r^3} \\ \theta(\tau) = \theta_0 \\ p_\theta(\tau) = p_{\theta0} \end{cases}
 \end{aligned} \tag{5.8}$$

We take $E = 0.995$, $L = 4.6$, $Q = 0.3$, initial angle $\theta_0 = \pi/2$, and integrate until the final time $t_f = 10^4$ by taking as basic scheme $\chi_h = \varphi_h^{[A]} \circ \varphi_h^{[B]} \circ \varphi_h^{[C]} \circ \varphi_h^{[D]} \circ \varphi_h^{[E]}$. In Fig. 5a we depict the error in phase space by varying r_0 in the interval $r_0 \in [9, 110]$ for methods $BM_6^{[4]}$, $BCM_6^{[4]}$ and the new processed methods $\hat{\psi}^{[6,4]}$ and $\hat{\psi}^{[8,4]}$. The step size is taken so that all the methods require the same

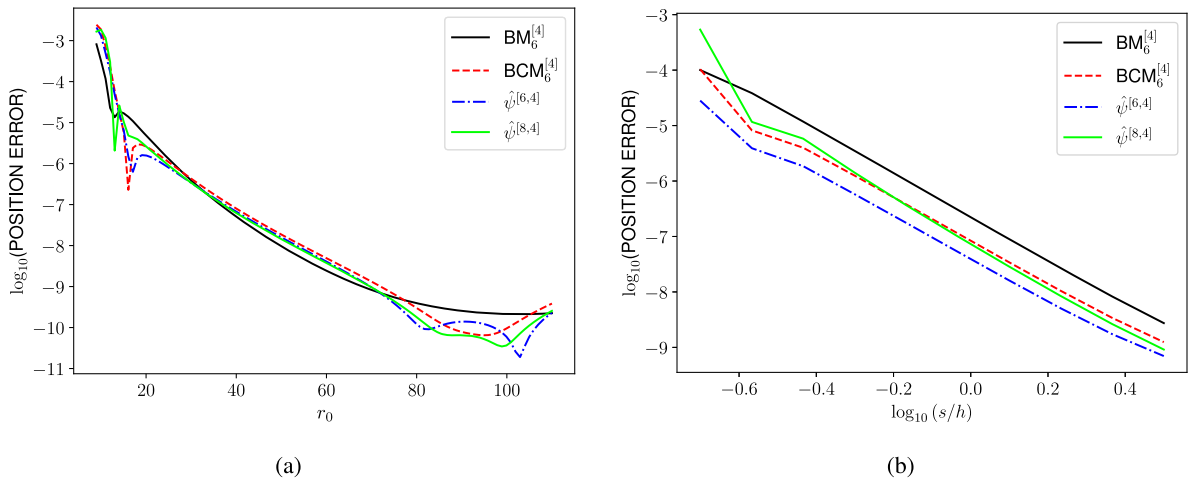


Fig. 5. Particle around Reissner–Nodström black hole. (a) Maximum position error for different values of the coordinate r_0 and for various 4th-order methods at the final time $t_f = 10^4$, evaluated with the same computational cost $s/h = 0.4$ (b) Efficiency diagram for different 4th-order methods with $r_0 = 18$ and the same t_f .

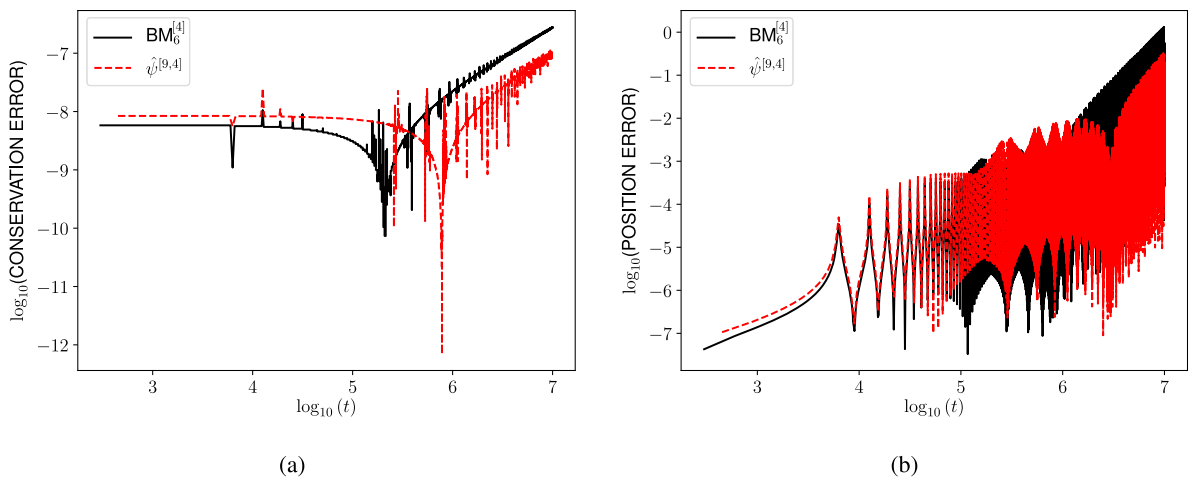


Fig. 6. Particle around Reissner–Nodström black hole. The evolution of the energy error (left) and position error (right) for $BM_6^{[4]}$ and $\hat{\psi}^{[9,4]}$. Both simulations are conducted with the same computational cost $s/h = 1$ and a step size $h < 10$.

computational effort. The right panel 5b shows the corresponding efficiency diagram, obtained with the same initial condition and $r_0 = 18$.

In addition to the improvement in the efficiency of processing methods with respect to standard compositions in this case, there is an important aspect to highlight. In [25], it is claimed that in these types of problems, roundoff errors grow and eventually lead to a drift in the conservation of the Hamiltonian when $h > 10$.

Our tests show that this phenomenon, although still present for processed methods, is delayed with respect to standard compositions, as illustrated in Fig. 6.

5.3. Motion of a charged particle under Lorentz force II

The effect of the ordering in the basic method χ_h is clearly visible e.g. in Fig. 4. We observe that, for some values of the parameter α , the error is up to 100 times smaller for the same scheme, and this may somehow conceal the potential advantages of one particular method with respect to others.

We should take into account, however, that the methods considered in this work are all based in compositions of an arbitrary first-order scheme χ_h and its adjoint χ_h^* , and not just on the Lie–Trotter splitting (5.6). It makes sense, then, to analyze the relative performance of the different methods on a given problem for another choice of χ_h . To do that, we consider again the problem (5.2) and take the explicit Euler method as χ_h , so that χ_h^* is given by the implicit Euler method. Fig. 7 collects the results achieved by 4th-order compositions and constitutes the analogous to Fig. 2. We see that the overall efficiency of the schemes essentially corresponds to what is expected based on the effective errors estimated in sections 3 and 4 and illustrated in the determination of traces for the

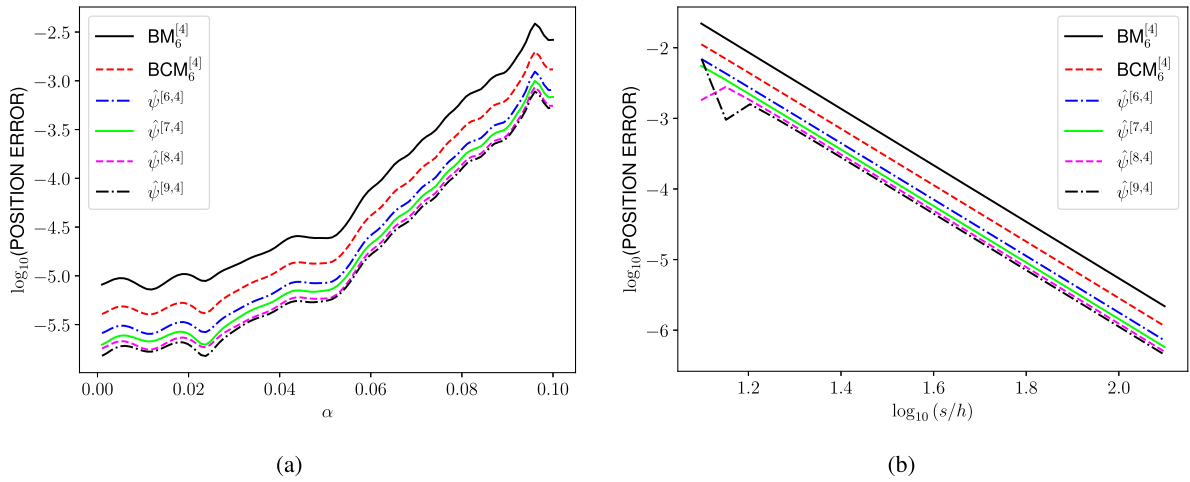


Fig. 7. Motion of a charged particle under Lorentz force. (a) Maximum position error for different values of the parameter α and for various 4th-order methods at the final time $t_f = 200$, evaluated with the same computational cost $s/h = 40$. χ_h and χ_h^* correspond to the explicit and implicit Euler methods, respectively. (b) Efficiency diagram for different 4th-order methods with $\alpha = 0.07$ and $t_f = 200$.

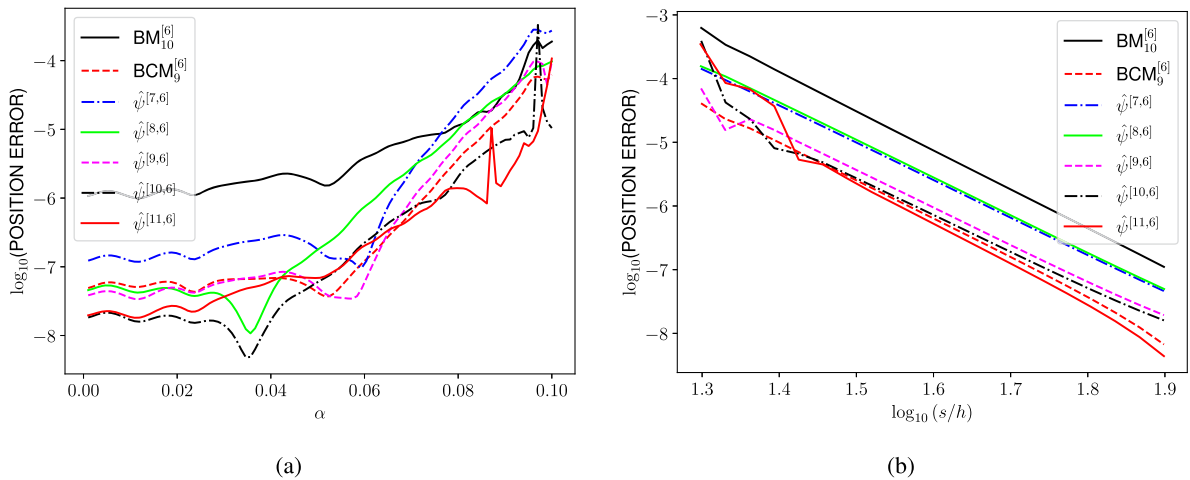


Fig. 8. Motion of a charged particle under Lorentz force. (a) Maximum position error for different values of the parameter α and for various 6th-order methods at the final time $t_f = 200$, evaluated with the same computational cost $s/h = 40$. Here χ_h and χ_h^* correspond to the explicit and implicit Euler methods, respectively. (b) Efficiency diagram for different 6th-order methods with $\alpha = 0.07$ and $t_f = 200$.

linear problem (3.3). Fig. 8 is obtained by 6th-order methods. The results achieved by interchanging the role of Euler explicit and Euler implicit are similar.

6. Concluding remarks

We have presented new families of processed splitting methods of order 4 and 6 especially designed to be applied to problems which can be separated into three or more parts, each of them being explicitly integrable. The construction strategy is as follows. First we determine the kernel, taking more stages than strictly required for solving the order conditions, so that the free parameters are chosen so as to minimize not only the first term in the asymptotic expansion of the truncation error, but also higher order terms, while keeping the size of the coefficients of the method reasonably small by keeping track of the 1-norm. The methods thus obtained are applied by computing the trace of the solution of a linear system defined by three different random matrices. This simple test allows us not only to check the effective order but also to discard schemes with large error constants. Second, for the most successful kernels we determine a particular processor π_h also as a composition of elementary maps, whereas its adjoint π_h^* is taken as an approximation for the inverse π_h^{-1} . In this way the overall integrator is still time-symmetric, leading to good preservation properties.

As the results gathered in Tables 5 and 7 show, increasing the number of stages allows one to get kernels with smaller effective errors and coefficients, the observed pattern closely following the rule of thumb formulated in [17]. Nevertheless, this efficiency pattern is not always followed when the methods are applied in practice, as shown by the examples collected here. This is specially

Table 9
Coefficients of processors for methods of order 4 and 6.

$\pi^{(9,4)}$	
$\beta_1 = -0.28566586026506785$	$\beta_2 = 0.015761586550701766$
$\beta_3 = -0.04362530065430363$	$\beta_4 = -0.03618407560045836$
$\beta_5 = 0.05244978481197771$	$\beta_6 = 0.28558661670075497$
$\beta_7 = 0.011677248456395364$	
$\pi^{(11,6)}$	
$\beta_1 = 0.2861698495034459$	$\beta_2 = 0.4134261834337682$
$\beta_3 = 0.10540576774873363$	$\beta_4 = -0.04664449698814812$
$\beta_5 = 0.05672335497036459$	$\beta_6 = 0.4990659695885505$
$\beta_7 = -0.3426195751795226$	$\beta_8 = 0.3464936779661353$
$\beta_9 = -0.23813674914660654$	$\beta_{10} = 0.24491881441628852$
$\beta_{11} = -0.49669544275221306$	$\beta_{12} = -0.3122980257722082$
$\beta_{13} = 0.03146400131096136$	$\beta_{14} = -0.030063016455253767$
$\beta_{15} = 0.31240611169589994$	$\beta_{16} = -0.10319811497811636$
$\beta_{17} = -0.42098894976942247$	$\beta_{18} = -0.283979022445134$
$\beta_{19} = -0.039440980719714046$	$\beta_{20} = -0.020860135690795974$
$\beta_{21} = 0.05463728247473808$	$\beta_{22} = -0.16673300456832169$
$\beta_{23} = 0.1509465011559501$	

true when the basic map χ_h is formed as a composition of the exact solution of each subproblem. On the contrary, if χ_h is a composition of first-order approximations, then the observed results agree nicely with the theoretical pattern.

A possible explanation for this behavior is related to the way the kernels are optimized. Specifically, in the optimization process carried out here, we have assumed that, for methods of order r , each Lie operator $E_{r+1,j}$, $j = 1, 2, \dots$ in the basis of Table 3 contributes equally to the error, but this not what always happens in practice. To see this point, let us consider a system that is separable into just two parts, say A and B , and the Hall basis for the corresponding free Lie algebra generated by A and B (similar considerations follow for any other Hall–Viennot basis [24]), which we denote as $\tilde{E}_{i,j}$. Then,

$$\tilde{E}_{1,1} = A, \quad \tilde{E}_{1,2} = B, \quad \tilde{E}_{2,1} = [A, B], \quad \tilde{E}_{3,1} = [A, [A, B]], \quad \tilde{E}_{3,2} = [B, [A, B]],$$

etc. Now, if we assume that the contribution of each $\tilde{E}_{r+1,j}$, $j = 1, 2, \dots$ to the error is similar, this is clearly not the case for the terms $E_{r+1,j}$, $j = 1, 2, \dots$ in previous basis of Table 3: in fact, for the 4th- and 6th-order methods, the elements $E_{r+1,1} = Y_{r+1}$, $r = 4, 6$ provide the smallest contribution to the error. On the other hand, if χ_h is taken as the explicit Euler method and the linear problem $\dot{U} = AU$ is considered, then

$$\chi_h = (I + hA) = \exp\left(hA - \frac{1}{2}h^2A^2 + \frac{1}{3}h^3A^3 + \dots\right)$$

so that $E_{n,1} = Y_n = (-1)^{n+1} \frac{1}{n} A^n$ and $E_{n,j} = 0$, $j > 1$, since $[Y_j, Y_k] = 0$. In consequence, the only surviving term at order $r + 1$ is $E_{r+1,1}$. Thus, for problems which are close to linear, when χ_h is taken as the explicit (or implicit) Euler method, we expect an important contribution from this term to the overall error. Notice that is the case for the examples examined here.

Acknowledgements

This work has been funded by Ministerio de Ciencia e Innovación (Spain) through project PID2022-136585NB-C21, MCIN/AEI/10.13039/501100011033/FEDER, UE, and also by Generalitat Valenciana (Spain) through project CIAICO/2021/180.

Appendix A

For reader’s convenience, we collect in Table 9 the coefficients for two particular processors:

$$\pi^{(9,4)} = \chi_{\beta_7 h}^* \circ \chi_{\beta_6 h} \circ \chi_{\beta_5 h}^* \circ \chi_{\beta_4 h} \circ \chi_{\beta_3 h}^* \circ \chi_{\beta_2 h} \circ \chi_{\beta_1 h}^*,$$

and

$$\pi^{(11,6)} = \chi_{\beta_{23} h}^* \circ \chi_{\beta_{22} h} \circ \dots \circ \chi_{\beta_2 h} \circ \chi_{\beta_1 h}^*,$$

corresponding to the kernels with $s = 9$ and $s = 11$ of effective order 4 and 6 of Tables 6 and 8, respectively.

References

[1] S. Blanes, M.P. Calvo, F. Casas, J.M. Sanz-Serna, Symmetrically processed splitting integrators for enhanced Hamiltonian Monte Carlo sampling, *SIAM J. Sci. Comput.* 43 (2021) A3357–A3371.
 [2] S. Blanes, F. Casas, *A Concise Introduction to Geometric Numerical Integration*, CRC Press, 2016.

- [3] S. Blanes, F. Casas, C. González, M. Thalhammer, Efficient splitting methods based on modified potentials: numerical integration of linear parabolic problems and imaginary time propagation of the Schrödinger equation, *Commun. Comput. Phys.* 33 (2023) 937–961.
- [4] S. Blanes, F. Casas, A. Murua, On the numerical integration of ordinary differential equations by processed methods, *SIAM J. Numer. Anal.* 42 (2004) 531–552.
- [5] S. Blanes, F. Casas, A. Murua, Composition methods for differential equations with processing, *SIAM J. Sci. Comput.* 27 (2006) 1817–1843.
- [6] S. Blanes, F. Casas, A. Murua, Splitting and composition methods in the numerical integration of differential equations, *Bol. Soc. Esp. Mat. Apl.* 45 (2008) 89–145.
- [7] S. Blanes, F. Casas, A. Murua, Splitting methods for differential equations, *Acta Numer.* (2024), in press.
- [8] S. Blanes, F. Casas, J. Ros, Symplectic integrators with processing: a general study, *SIAM J. Sci. Comput.* 21 (1999) 711–727.
- [9] S. Blanes, P.C. Moan, Practical symplectic partitioned Runge–Kutta and Runge–Kutta–Nyström methods, *J. Comput. Appl. Math.* 142 (2002) 313–330.
- [10] J.C. Butcher, J.M. Sanz-Serna, The number of conditions for a Runge–Kutta method to have effective order p , *Appl. Numer. Math.* 22 (1996) 103–111.
- [11] E. Hairer, C. Lubich, G. Wanner, *Geometric Numerical Integration. Structure-Preserving Algorithms for Ordinary Differential Equations*, second ed., Springer-Verlag, 2006.
- [12] E. Hairer, S. Nørsett, G. Wanner, *Solving Ordinary Differential Equations I, Nonstiff Problems*, second revised ed., Springer-Verlag, 1993.
- [13] Y. He, Y. Sun, J. Liu, H. Qin, Volume-preserving algorithms for charged particle dynamics, *J. Comput. Phys.* 281 (2015) 135–147.
- [14] Y. He, Y. Sun, J. Liu, H. Qin, Higher order volume-preserving schemes for charged particle dynamics, *J. Comput. Phys.* 305 (2016) 172–184.
- [15] M.A. López-Marcos, J.M. Sanz-Serna, R.D. Skeel, Explicit symplectic integrators using Hessian-vector products, *SIAM J. Sci. Comput.* 18 (1997) 223–238.
- [16] R.I. McLachlan, On the numerical integration of ODE's by symmetric composition methods, *SIAM J. Sci. Comput.* 16 (1995) 151–168.
- [17] R.I. McLachlan, Families of high-order composition methods, *Numer. Algorithms* 31 (2002) 233–246.
- [18] R.I. McLachlan, R. Quispel, Splitting methods, *Acta Numer.* 11 (2002) 341–434.
- [19] R.I. McLachlan, Tuning symplectic integrators is easy and worthwhile, *Commun. Comput. Phys.* 31 (2022) 987–996.
- [20] H. Munthe-Kaas, B. Owren, Computations in a free Lie algebra, *Philos. Trans. R. Soc. Lond. A* 357 (1999) 957–981.
- [21] J.M. Sanz-Serna, M.P. Calvo, *Numerical Hamiltonian Problems*, Chapman & Hall, 1994.
- [22] M. Suzuki, Fractal decomposition of exponential operators with applications to many-body theories and Monte Carlo simulations, *Phys. Lett. A* 146 (1990) 319–323.
- [23] V.S. Varadarajan, *Lie Groups, Lie Algebras, and Their Representations*, Springer-Verlag, 1984.
- [24] G. Viennot, *Algèbres de Lie Libres et Monoïdes Libres*, *Lecture Notes in Mathematics*, vol. 691, Springer-Verlag, 1978.
- [25] Y. Wang, W. Sun, F. Liu, X. Wu, Construction of explicit symplectic integrators in general relativity. I. Schwarzschild black holes, *Astrophys. J.* 907 (2021) 66.
- [26] Y. Wang, W. Sun, F. Liu, X. Wu, Construction of explicit symplectic integrators in general relativity. II. Reissner–Nordström black holes, *Astrophys. J.* 909 (2021) 22.
- [27] J. Wisdom, M. Holman, J. Touma, Symplectic correctors, in: J. Marsden, G. Patrick, W. Shadwick (Eds.), *Integration Algorithms and Classical Mechanics*, in: *Fields Institute Communications*, vol. 10, American Mathematical Society, 1996, pp. 217–244.
- [28] H. Yoshida, Construction of higher order symplectic integrators, *Phys. Lett. A* 150 (1990) 262–268.